

A V Krasilnikov et al

Study of D–T Neutron Energy Spectra at JET using Natural Diamond Detectors

"This document is intended for publication in the open literature. It is made available on the understanding that it may not be further circulated and extracts may not be published prior to publication of the original, without the consent of the Publications Officer, JET Joint Undertaking, Abingdon, Oxon, OX14 3EA, UK".

"Enquiries about Copyright and reproduction should be addressed to the Publications Officer, JET Joint Undertaking, Abingdon, Oxon, OX14 3EA".

Study of D–T Neutron Energy Spectra at JET using Natural Diamond Detectors

A V Krasilnikov¹, V N Amosov¹, P van Belle,
O N Jarvis, G J Sadler.

JET Joint Undertaking, Abingdon, Oxfordshire, OX14 3EA,
¹Troitsk Institute for Innovating and Fusion Research (TRINITI), Troitsk, Russia.

Preprint of a Paper to be submitted for publication in
Plasma Physics and Controlled Fusion

September 2000

ABSTRACT

Four Natural Diamond Detectors (NDD) have been used for deuterium - tritium neutron spectrometry and flux monitoring during the 1997 tritium experiments (DTE1) carried out in the Joint European Torus (JET).

Neutron energy spectra have been measured with three NDDs for discharge scenarios that included: (a) hot ion H-mode studies using combined NB and ICRF heating, (b) optimized shear experiments using combined NB and ICRF heating, (c) alpha - particles heating experiments with NB heating only and (d) ICRF heating studies without NB heating. Within the statistical accuracy of the data, the spectra for high performance discharges can be adequately represented by Gaussian distributions, whose *fwhm* values provide effective ion temperatures that characterize the energy distributions of the ions taking part in fusion reactions.

The performance of the miniature diamond detectors for neutron spectrometry is evaluated through comparison with the results obtained from the major d-t neutron spectrometers installed at JET.

1. INTRODUCTION

Deuterium-tritium (d-t) experiments using high-power neutral-beam injection (NBI) and ion cyclotron resonance heating (ICRH) were carried out at the Joint European Torus (JET) in 1997 [1]. During these experiments, up to 16 NBI sources (two banks of 8) injected neutral particles at angles $\sim 58 \pm 6^\circ$ to the axis of the plasma current (in the co-direction). The total beam power reached 23 MW, being comprised of deuterium beams at 80 keV and/or tritium at 155 keV. Many of these discharges employed combined NBI and ICRF heating. Several ICRF-only heating schemes were investigated; for some of these schemes the fluxes of 14 MeV neutrons were sufficiently high that d-t neutron spectrometry could be used to study the fast deuterium and tritium energy distributions.

During the high fusion power phases of JET optimized shear discharges, plasma-plasma (thermal) neutron production sometimes exceeds the beam-plasma neutron production and measurements of the neutron energy distributions directly reflect the bulk ion temperature and the plasma toroidal rotation rate. However, when beam-plasma neutron production is strong, measurements of the neutron emission intensity and of the neutron energy spectra reflect mainly the energy distributions of the slowing-down beam ions. During ICRF heating, the d-t neutron intensity and energy distributions reflect the efficiency of resonant and non-resonant particle heating, in a manner that depends upon the heating scheme. Finally, d-t neutron energy distributions provide direct information on the alpha-particle birth energy distributions and might be expected to provide a clear demonstration of alpha-particle heating of the plasma ions during the highest performance discharges. In all d-t discharges, the relative proportions of deuterium and tritium in the plasma core are important and can be investigated using neutron spectrometry.

The present paper reports measurements of 14-MeV neutron fluxes and of neutron energy spectra obtained during the JET DTE1 experiment using very small natural diamond detectors. Diamond detectors are far superior to silicon diodes for recording very high fluxes of d-t neutrons on account of their greater radiation damage tolerance. In terms of detection efficiency and intrinsic energy resolution they appear, at first sight, to be competitive with the large purpose-built 14-MeV neutron spectrometers already deployed at JET. However, due to incomplete charge-collection, the diamond pulse-height spectra exhibit low-energy tails that are large enough to be troublesome when investigating very broad neutron energy spectra, as was mostly the situation in this work; consequently, the diamond spectrometer results were of lower quality than those from the three major spectrometers. It is likely that analysis of the diamond spectra would have been more satisfactory had more detailed detector response functions been available. The unquestioned advantages of the diamonds are that they make fewer demands on space and are vastly easier to install and operate than the major spectrometers.

2. DIAGNOSTIC ARRANGEMENT

The Natural Diamond Detectors (NDD) were developed in the Russian Federation [2-4]. Their application to neutron spectrometry is based on the large charge collection distance (several mm) for selected natural diamonds. In the case of d-t neutron spectrometry, the $^{12}\text{C}(n,\alpha_0)^9\text{Be}$ reaction (leaving the ^9Be nucleus in its ground-state) provides a pulse height spectrum containing a very narrow, well-separated, peak corresponding to the 14 MeV neutrons. The full width at half maximum (*fwhm*) of the $^{12}\text{C}(n,\alpha_0)^9\text{Be}$ line of the NDD pulse height spectrum recorded during a JET plasma discharge is a measure of the broadening of the energy distribution [5,6] of those d-t neutrons which leave the plasma along a direct line-of-sight leading to the detector. In general, the *fwhm* can be interpreted as either a real or just an effective ion temperature T_{eff} , depending on circumstances. For clarity, we henceforth use the expression “neutron temperature”, rather than effective temperature, as a reminder of the weighting arising from the reactivity, $\langle\sigma v\rangle$, of the d-t fusion reaction cross-sections. The neutron energy corresponding to the mean position of the line is a measure of both the total energy of the ions taking part in the reaction and the average velocity of the centres-of-mass of the reacting d and t ions towards the detector. Consequently, the mean energy contains information about the bulk plasma rotation rate.

The high energy resolution offered by the NDD detectors, coupled with the high radiation resistance of diamonds (5×10^{14} n/cm²), were the essential conditions that permitted their successful application as d-t neutron spectrometers and flux monitors in the high radiation environment of the JET deuterium-tritium (DTE1) experiment. Neutron spectra for the detectors using nearly mono-energetic neutrons were obtained from a d-t neutron generator [7]. The intrinsic resolution for the full-energy line is usually well described by a gaussian with *fwhm* of between 2 and 3%, although NDD5 exhibited the best value yet recorded of 1.2%. Such energy resolutions are sufficiently good that there is little instrumental broadening of fusion neutron spectra provided

these are narrow, but for broad spectra the low energy tail due to incomplete charge collection becomes important. Unfortunately, complete sets of response functions (i.e. using a number of different energies for the incident mono-energetic neutrons) were not obtained, so accurate unfolding of very broad energy spectra (typical of high neutron yield discharges) was not possible. Consequently, for these high performance discharges, it was necessary to represent the fusion neutron spectra by Gaussian distributions, a reasonable assumption in the circumstances.

Table 1. Detector dispositions and efficiencies

Detector	View of plasma	Application (resolution)	Ratio of flux at detector to total neutron production rate, cm^{-2}	Sensitivity, ratio of counts to d-t flux at detector, $\text{counts}/(\text{n}/\text{cm}^2)$
NDD1	Tangential	Spectrometer (2.5%) Counter	$1.8 \cdot 10^{-11}$	$1.25 \cdot 10^{-5}$ $5.0 \cdot 10^{-4}$
NDD2	Global	Counter	$5 \cdot 10^{-8}$	$1.3 \cdot 10^{-4}$
NDD4	Tangential	Spectrometer (2.1%) Counter	$1.8 \cdot 10^{-11}$	$1.67 \cdot 10^{-5}$ $6.7 \cdot 10^{-4}$
NDD5	Vertical	Spectrometer (1.2%) Counter	$2.8 \cdot 10^{-11}$	$1.75 \cdot 10^{-5}$ $5.3 \cdot 10^{-4}$

Three detectors were used as spectrometers. Their compact size ($\sim 1 \text{ cm}^3$ overall) allowed them to be installed within or behind neutron collimators established for other detectors and spectrometers, all of which were outside the biological shielding walls of the JET Torus Hall, without interfering with the performance of those systems. The dispositions and efficiencies of the diamond detectors are listed in Table 1.

Two detectors (NDD1 and NDD4) were installed close together at a distance of 20 m from the plasma behind the proton recoil telescope neutron spectrometer (PRTel [8]) collimation system. The PRTel views the JET plasma along horizontal line-of-sight 15 cm below the equatorial plane of the plasma and at an angle of 52° with respect to the current axis (Fig.1). For simplicity, this viewing direction will be referred to as being “tangential”, although “quasi-tangential” would be more accurate. The count-rates were quite modest because of the small solid angle subtended by the plasma, defined as a 0.10 m diameter chord passing through the plasma and

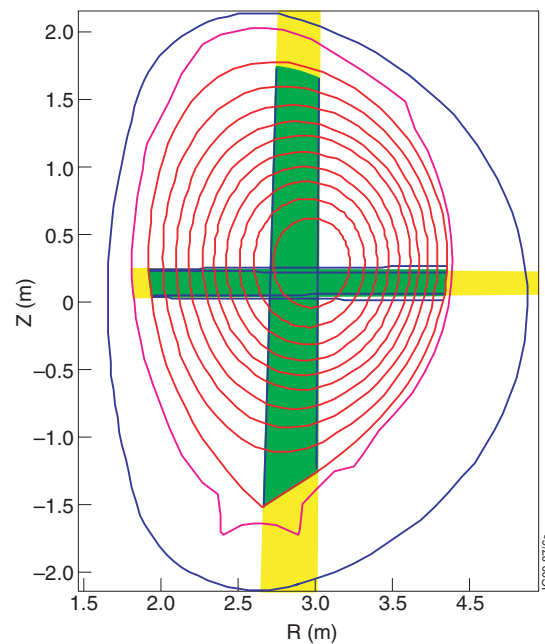


Fig.1: Illustrating the solid angles along which the NDD5 (vertical) and NDD1 and NDD4 (tangential) d-t neutron spectrometers view the JET plasmas.

a 20 m plasma-to-detector separation. Thus, detector NDD4 when used as a (collimated) flux monitor achieved a maximum count-rate of only $6.8 \cdot 10^4$ counts/s during the discharge number 42976, which provided the record DT neutron production rate of $5.7 \cdot 10^{18}$ n/s.

The third detector (NDD5) was installed inside a vertical neutron collimator (diameter 0.02 m, length between collimator entrance and detector 1.2 m) at a distance of 17 m above the plasma. It thus measured a neutron spectrum corresponding to emission normal to the equatorial plane and is therefore insensitive to the plasma toroidal rotation (see Fig.1).

The signals from all three detectors were fed into standard Ortec spectroscopy electronics modules, comprising model 142A preamplifiers and model 673 spectroscopy amplifiers operating with shaping times of 0.25 μ s. The total count rate in each of the NDD-based spectrometers did not exceed $8.5 \cdot 10^4$ counts/s, so there was no need to employ signal pile-up rejection techniques.

A fourth, unshielded, detector (NDD2) was installed inside the Torus Hall in the equatorial plane of the torus at a distance of only 3 m from the plasma axis to monitor the total d-t neutron production rate with good statistical accuracy. The signals from NDD2 were fed, without pre-amplification, via a 150 m long cable to special-purpose fast counting electronics. The duration of the current pulse from a diamond detector is approximately 3 ns, while the rise-time associated with the transmission cables is about 15 ns. Thus, this detector could be operated in counting mode at rates of over 10^7 counts/s. Count rates due to d-t neutrons of up to $6.7 \cdot 10^5$ s⁻¹ were recorded, corresponding to total event rates of up to $8.3 \cdot 10^7$ s⁻¹ (mostly generating trivially small signals). The detector suffered two abrupt changes in efficiency during the course of the DTE1 experiment, the first being a sudden drop by about 15%, followed some weeks later by an equally abrupt recovery. These events are attributed changes at the electrical contact on the diamond surface. The detector displayed no changes attributed to the radiation dose received during the DTE1 campaign, despite accumulated fluences of $\sim 1.2 \cdot 10^{13}$ n/cm² due to unscattered d-t neutrons, $\sim 1.2 \cdot 10^{13}$ n/cm² down-scattered neutrons and $\sim 1.2 \cdot 10^{13}$ γ /cm².

3. D-T NEUTRON RATE MONITORING

The 2.5 MeV neutrons from d-d fusion reactions only deposit energy within the diamond detectors through elastic scattering, producing ¹²C recoil particles with energies up to 0.8 MeV [4]. Gamma rays with energies of up to several MeV produce Compton electrons with an exponentially decaying energy spectrum [6]. For monitoring d-t neutron with optimum efficiency in a mixed field of d-t neutrons, d-d neutrons and gamma rays, the low level discriminator for NDD5 was set at 1.7 MeV, permitting 50% of all events produced by d-t neutrons to be recorded with negligible contributions from the other sources. The discriminator settings were determined using standard alpha-particle sources.

As described above, NDD4 (in parallel with spectrometry) and NDD2 were used for d-t neutron rate monitoring. NDD4 was well collimated and thus was biased to sample the d-t emissivity at the centre of the plasma. As the gamma flux at this detector position was very low,

its low-level discriminator was set at 1.2 MeV, permitting 56% of all events produced by d-t neutrons to be recorded. NDD2 was uncollimated and unshielded, viewing directly a large volume of plasma and sensitive to both wall-scattered neutrons and neutron capture gamma rays. The sensitivities of this detector to d-t, d-d neutrons and gamma rays are $1.3 \cdot 10^{-4}$, $1.6 \cdot 10^{-4}$ counts/(n/cm²) and $\sim 1.6 \cdot 10^{-4}$ counts/(γ /cm²), respectively. However, because of its exposed location, the low level discriminator was set close to the energy of the $^{12}\text{C}(n,\alpha_0)^9\text{Be}$ line, reducing its potential efficiency by about a factor of 100.

The time evolutions of the d-t neutron count rate from the central region of the plasma and of the total neutron emission rate as measured with NDD4 and NDD2 during a shot with strong sawtooth oscillations are shown in Fig.2. The considerable reduction of d-t neutron emissivity in the core following a sawtooth crash, usually attributed to particle mixing and redistribution, is clearly seen. The absolute calibration for the uncollimated NDD2 was obtained by normalization to the signal derived from the fission chambers, the standard diagnostic for neutron yield measurements at JET [9]; the time evolution recorded by NDD2 was in excellent agreement with that of the fission chambers.

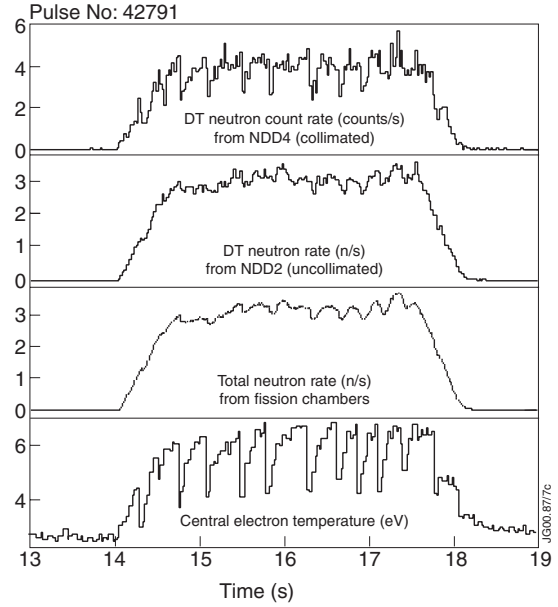


Fig.2: Comparing the time evolutions of the line-integrated d-t neutron signal (primarily sampling the central region of the plasma) measured with the collimated detector NDD4 (top frame) with the global signal recorded with the uncollimated detector NDD2 and the fission chambers; the central electron temperature is also shown. The discharge illustrated exhibited strong sawtooth activity.

4. NEUTRON ENERGY SPECTRA

For a Maxwellian d-t plasma with ion temperature T , the d-t neutron spectrum has a Gaussian shape [10]:

$$f(E_n) = (2\pi\sigma_E)^{-0.5} \exp[-(E_n - \langle E_n \rangle)^2 / 2\sigma_E^2] \quad (1)$$

where σ_E is the standard deviation. The fwhm is given by $\Delta E_n = [8 \times \ln(2)]^{0.5} \sigma_E$. For plasmas with ion temperatures in the range 20-30 keV,

$$\Delta E_n = 178 \times T^{0.5} \quad (2)$$

where ΔE_n and T are in kilo-electron-volts.

The ion component in JET plasmas contains thermal ions, fast beam ions and ions accelerated by ICRH. Neutrons are produced from three reaction channels: thermal (i.e. plasma-plasma), fast ion (beam and/or ICRH accelerated) - plasma and beam-beam. The relative importance of the three channels depends on plasma parameters and applied heating conditions.

Beam-beam neutron production was very low during the DTE1 experiments because the beams were not well focused at the plasma axis.

For almost all of the DTE1 discharges, the neutron energy spectra could be fitted adequately using a Gaussian distribution. This does not, in general, imply that the ion energy distribution is Maxwellian but, without further information, we cannot prove that it is not. Nevertheless, it is convenient to apply equ. (2) in order to deduce the neutron temperature, i.e. one that is weighted by the reactivity, $\langle\sigma v\rangle$, of the d-t fusion reaction. In the case of ICRF heating, it is conventional to represent the ion energy distribution in terms of a two-dimensional Maxwellian for the RF-accelerated ions superimposed upon an isotropic thermal background. The velocity distributions of slowing down beam ions are not isotropic, so here also we have to consider a two-dimensional energy distribution (but not Maxwellian). Clearly, neutron spectra obtained for the vertical and tangential lines-of-sight at JET will yield different neutron temperatures (T_{Vert} and T_{Tang}). For ICRF heating, where the perpendicular fast ion temperature T_{\perp} may greatly exceed the parallel temperature T_{\parallel} , both spectra will be determined mainly by the perpendicular velocity distributions of the fast ions: the vertical neutron temperature T_{Vert} will sample only T_{\perp} , whereas the tangential neutron temperature T_{Tang} will sample $(\cos^2 52 \times T_{\parallel} + \sin^2 52 \times T_{\perp} \approx \sin^2 52 \times T_{\perp})$.

4.1 Typical energy spectra from high-performance discharges

The highest fusion powers were produced during hot ion H-mode experiments, with applied powers of up to 22.8 MW NBI and between 3 and 6 MW of ICRH. Typically, the plasma electron density increased almost linearly from 2 up to $5 \times 10^{19} \text{ m}^{-3}$ during the NB heating period. Figures 3 and 4 show pulse height spectra obtained with detectors NDD4 and NDD5 (tangential and vertical positions, respectively) during 1 and 0.9 second of the high fusion power phase of the discharge number 42976 (the highest fusion power discharge). The $^{12}\text{C}(n, \alpha_0)^9\text{Be}$ lines of these spectra represent the energy distribution of d-t neutrons leaving the plasma at an angle of 52° and 90° , respectively, to the current axis direction. The broadening of these distributions and the shift of the NDD4 peak from 14.02 MeV depend upon the ion energy distributions and the toroidal rotation of the plasma. For a uniformly rotating Maxwellian plasma, the shift ΔE_n of the d-t neutron peak position is connected with the velocity of the plasma toroidal rotation by the relation

$$\Delta E_n(\text{rot}) \approx 5.6 \times 10^{-4} \langle V \rangle \cos 52^\circ, \quad (3)$$

where ΔE_n in keV and $\langle V \rangle$ in m/s. In addition, for a Maxwellian plasma there is a shift attributable to the ion temperature, which from Brysk [10] can be expressed as

$$\Delta E_n(T_i) \approx (3/10) \times T_i + (T_i)^2 (\partial/\partial T_i) [\ln (T_i^{2/3} \langle \sigma v \rangle)] \quad (4)$$

For $T_i = 10 \text{ keV}$, $\langle \sigma v \rangle \sim T_i^{2.5}$ for d-t reactions at a temperature of 10 keV. Approximately, the shift is $3 T_i$, and is not negligible in comparison with the rotation shifts encountered during the high performance DTE1 discharges. For non-Maxwellian plasmas, with which we are mostly

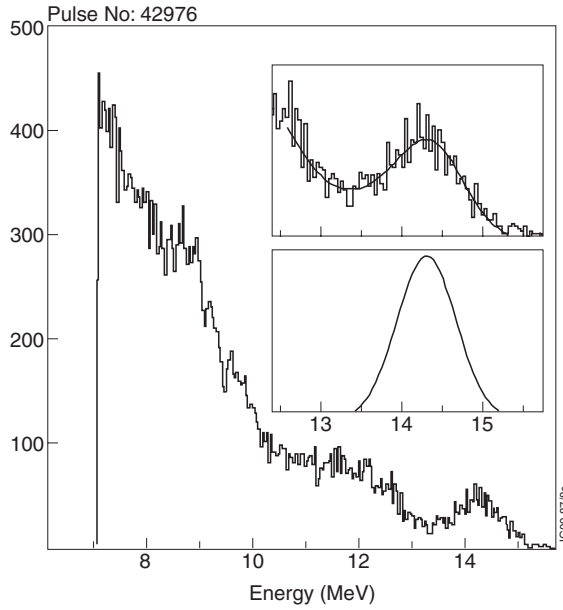


Fig.3: NDD4 (tangential) pulse height spectrum accumulated during 1 second (12.5 to 13.5s) of the JET record fusion power plasma shot 42976. The insert shows a gaussian fit (upper plot) to the full energy line, and (lower plot) the assumed Gaussian spectrum superimposed on a weak background; the neutron temperature is 23.5 ± 4.5 keV and the mean neutron energy 14.300 ± 0.018 MeV.

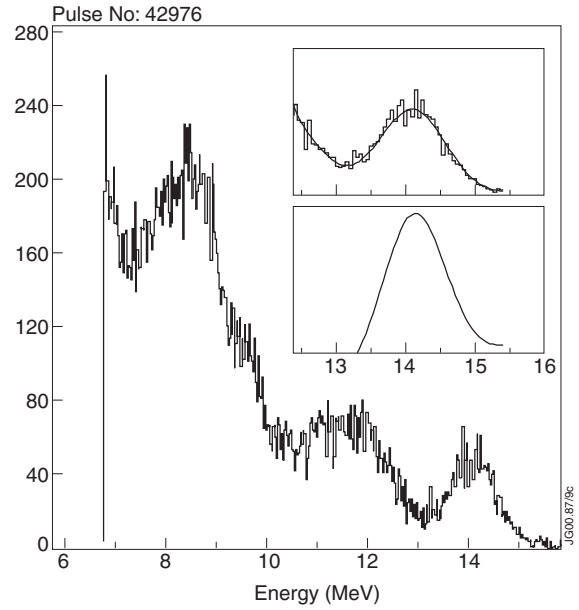


Fig.4: NDD5 (vertical) pulse height spectrum accumulated during 0.9 second (12.6 to 13.5 s) of the JET record fusion power discharge 42976. The insert shows a Gaussian fit (upper plot) to the full energy line, and (lower plot) the assumed Gaussian spectrum superimposed on weak background; the neutron temperature is 35.1 ± 3.0 keV and the mean energy 14.122 ± 0.015 MeV.

concerned, a full kinematics calculation must be performed in order to derive the temperature shift. A Monte Carlo code is available for this purpose [11]. Thus, although the neutron spectra from the diamond detectors provide clear evidence of the shifts in the mean energy of the fusion neutrons, the derivation of reliable plasma rotation rates from the data involves considerable computational effort.

The upper plots show in the insets in figs. 3 and 4 show the quality of the fits to the portion of the neutron spectra above the (n,α_1) peak and containing the important feature of the (n,α_0) peak. The fitting procedure used to produce these figures involves a least-squares fitting of a Gaussian distribution representing the energy spectrum of the neutrons folded into the response function of the relevant diode, as measured with mono-energetic neutrons. Unfortunately, this was not sufficient to fit the data adequately. Consequently, the fitting routine introduced an additional sloping low-energy background component that would normally represent neutrons that have lost energy through scattering processes either in the tokamak vacuum vessel or while travelling along the neutron collimators. However, in the present case, this contribution is small and goes negative, indicating that the representation of the detector response function could be improved. The deduced Gaussian superimposed on the fitted background is shown in the lower of the plots in the insets to figs. 3 and 4. Provided the statistical accuracy is good, this procedure produces satisfactory results. Usually, the statistical accuracy is poor, when it is found necessary instead to fit a Gaussian on top of a sloping background to the raw data above the minimum to

the low energy side of the (n, α_0) peak; the background function now includes the main features of the detector response. In this case, the precise neutron temperature derived depends on the assumptions made about the shape of the background so the uncertainties attributed to the neutron temperature must take this variation into account. These uncertainties are sometimes appreciably larger than the purely statistical errors generated by the fitting process for the assumed (precise) background function.

4.2 Fast ion energy estimation with NBI dominant

Just after the start of NBI and before the injected ions have had time to settle into their steady-state energy distribution, the d-t neutron energy spectra should display a broadening that is simply determined by the injection energy of the fast beam ions and a shape that is characteristically hollow, with prominent low and high energy shoulders (as illustrated in fig. 5). The perpendicular energies of the beam particles can be estimated from the measured shifts of the shoulder maxima from the mean energy of the d-t neutrons, assuming the beam ion velocities to be much greater than the plasma ion velocities. In this case, the values of the energy shifts of the shoulders are related to the averaged perpendicular energy as

$$\Delta E_n = 67.1 (E_{\perp d})^{0.5} \text{ for d beam - T plasma neutrons} \quad (5)$$

and

$$\Delta E_n = 82.2 (E_{\perp t})^{0.5} \text{ for t beam - D plasma neutrons} \quad (6)$$

where ΔE_n , $E_{\perp d}$ and $E_{\perp t}$ are in keV. For spectra obtained using a vertical-viewing spectrometer, we have $E_{\perp} = E_{\text{beam}} \times \sin^2 58$ to allow for the beam-injection angle.

It is of interest to examine suitable discharges to discover the extent to which the measured spectra display this feature. A suitable plasma discharge scenario was offered by the ρ^* scaling experiments [11] which used 20 MW of NBI and 2 to 4 MW of ICRF heating, resulting in ELMy H-mode discharges with electron densities rising during NBI from 4 up to $8 \times 10^{19} \text{ m}^{-3}$ and ion temperatures reaching only 6 keV. The vertical line-of-sight is necessary for such an investigation as the resulting spectra are insensitive to plasma rotation and to considerations of co-passing as opposed to counter-passing beam ions.

Figure 5 shows the perpendicular d-t neutron spectra accumulated during the first 0.3 seconds of beam-injection and during the following 0.6 s, summed over five similar discharges for improved statistics (numbers 42810, 42811, 42812, 42820, 42821). The neutron energy distribution has a distinctly non-Gaussian structure at the beginning of NBI, but becomes approximately Gaussian soon after. The form of the upper curve suggests that shoulders in the spectra are seen, but the statistics are too poor to draw firm conclusions. The spectrum has been analyzed in terms of the three major components, a narrow thermal contribution, a broader d-

beam, T-plasma contribution (76 keV deuterium injection) and a very broad t-beam D-plasma emission contribution (155 keV tritium injection) that is quite small in these predominantly tritium plasmas. A Monte-Carlo kinematics code [12] has been used for these calculations. To exaggerate the effect sought, the slowing down of the beam ions has been ignored for the first of the spectra (the upper pair of plots). Although the shoulders are evident in the underlying neutron spectra, it is evident that they have been entirely lost in the process of folding with the detector response function (the fitted solid line in the top picture). The spectrum for the second time interval, for which a slowing-down beam energy distribution was used, shows the combined effect of an increased thermal contribution and the filling of the hollow in the beam-plasma spectrum as equilibrium fast ion energy distribution is established.

During steady-state conditions, the total broadening of the d-t neutron energy spectra when beam-plasma neutron emission is dominant will depend upon the relative intensities of the t beam - D plasma and d beam

- T plasma contributions. The broadening of the perpendicular neutron spectra was indeed observed to be greater in experiments with preponderant t beam - D plasma neutron production. In general, interpretation of neutron spectra involves use of a computer code to predict the relative contributions from the several d-t neutron production channels and then the application of the Monte-Carlo kinematics code [12] to compute the spectra from each of these contributions, taking into account the full slowing-down beam ion energy distributions. Finally, the summed neutron spectrum has to be folded with the detector response function for comparison with the observed spectrum broadening, which will usually be much greater than the purely thermal broadening. For example, the (Gaussian) broadening of the perpendicular neutron spectrum accumulated with NDD5 during NBI for five discharges (42993, 43002, 43003, 43004, and 43005) of the ρ^* scaling experiments (about 12 MW of pure tritium NBI) was 1007 ± 30 keV, indicating a neutron temperature of 32 keV, whereas the measured temperature of the thermal

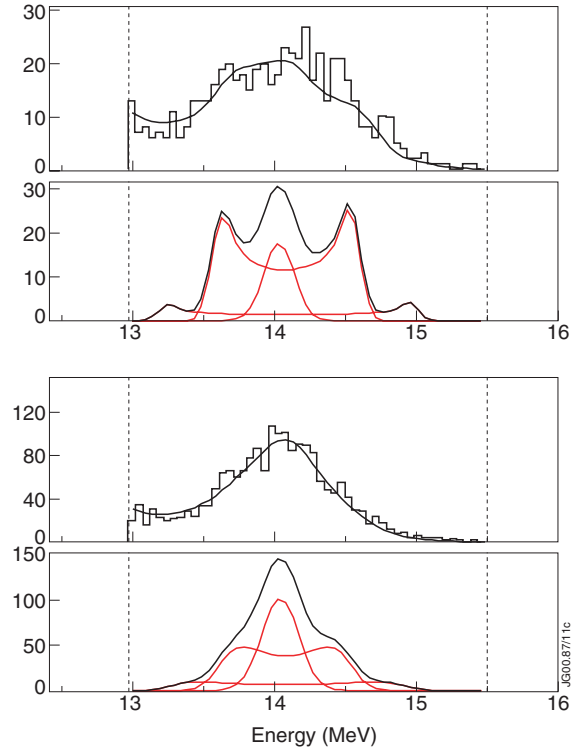


Fig. 5: Upper pair: Perpendicular d-t neutron spectrum (NDD5) accumulated during the first 0.3 s of five similar discharges with comparable powers of 76 keV deuterium and 155 keV tritium injected into relatively cold (2 keV) and dense ($6 \times 10^{19} \text{ m}^{-3}$) tritium-rich DT plasmas. The three main components of the neutron spectrum are shown underneath, assuming mono-energetic beam ions; the curve fitted to the data points is the spectrum folded into the detector response function. Lower pair: As above, but for the 0.6 s period immediately following the first frame. For this longer period, the full slowing down beam ion distribution is adopted and the plasma temperature has risen.

ions was just 4 keV. The fact that the spectrum broadening depends on the beam injection energies and on the deuterium/tritium mix can be usefully exploited as a means of determining the D/T fuel density ratio in the plasma core.

4.3 Fast ion energy estimation with ICRH

Experiments with deuterium minority ICRH (28 MHz, and 3.8T toroidal field) in tritium plasma were performed with the ICRH powers equal to 4, 4.7 and 6 MW. During deuterium minority heating, the RF energy goes mainly into perpendicular motion and these fast deuterons interact with relatively cold plasma tritons to produce d-t neutrons. The ion temperature measured by Charge-Exchange Recombination Spectroscopy (CXRS) was 6.5 keV. In this case, the d-t neutron spectrum broadening is determined by the RF-accelerated deuteron energy distribution weighted by the fusion reaction cross-section. The fast ion energy distribution is described as the product of two exponentials, representing the parallel and perpendicular energy components, of which the latter is larger and of most interest. The width of the perpendicular energy distribution can then be written as:

$$\Delta E_{n\perp} = 178 [(m_d E_{d\perp} + m_t E_{t\perp}) / (m_d + m_t)]^{0.5} \quad (7)$$

where $\Delta E_{n\perp}$ is the perpendicular fwhm broadening of the d-t neutron spectrum in keV, $T_{d\perp}$ and $T_{t\perp}$ are the deuteron and triton perpendicular temperatures in keV, and m_d and m_t are deuteron and triton masses. The term inside the parentheses is the effective temperature of distribution containing two particle species at different temperatures as given by Brysk [10], with E_{\perp} substituted for T , as appropriate for a Maxwellian plasma. The perpendicular and tangential neutron temperatures obtained with NDD4 and NDD5 are $T_{\text{Vert}} \approx 50$ keV and $T_{\text{Tang}} \approx 30$ keV, showing a small but measurable increase with ICRH power. The ‘‘tangential’’ deuteron effective temperatures are approximately equal to the corresponding values of perpendicular deuteron effective temperatures multiplied by $\sin^2 52^\circ$, as expected. Applying the simple relationship (7) leads to an estimate for the RF-accelerated deuteron effective perpendicular energy E_{\perp} of ≈ 115 keV.

5. COMPARISON OF SPECTROMETER PERFORMANCE

The performance of the diamond detectors as neutron spectrometers is best examined by comparison with results obtained with the three major spectrometers installed at JET. These are:-

- the time-of-flight, associated particle, spectrometer (TANSY, [13]) installed in the Roof Laboratory and therefore viewing the plasma from a vertical direction (a line-of sight similar to that used for the diamond detector NDD5),
- the tandem-radiator proton recoil telescope spectrometer (PRTel [8]), whose line-of-sight was used for diamond detectors NDD1 and NDD4,

- a magnetic analysis proton-recoil spectrometer (MPR [14],[15]) close-coupled to the tokamak and viewing the plasma along a tangential line-of-sight similar to that of PRTel except that it passes through the plasma centre instead of 15 cm below.

TANSY offers an energy resolution that depends on the thickness of its polyethylene target foil; for most of DTE1 the resolution was set at 1.6%, at the cost of a lowered efficiency - comparable with that of the NDD5 diamond detector. It does not exhibit a low energy tail but instead suffers from an energy-independent background due to random coincidences in the various detectors.

The PRTel offers 2.2% energy resolution and an efficiency of several times better than the diamonds. It also exhibits a low-energy tail, much smaller than those from the diamonds, but which nevertheless has to be included in the spectrometer response function if unambiguous spectrum unfolding is to be achieved.

The MPR also offers a resolution that depends on the thickness of its polyethylene target foil; it was set at 4% (perfectly adequate for the broad energy spectra under study in this paper). It has an exceptionally high sensitivity due to its position close to the tokamak, so that its response is two orders of magnitude greater than those of the other spectrometers. It exhibits a low energy tail, but one that is even smaller than that for the PRTel.

The performance of the diamond detectors has been compared with that of the mainstream spectrometers during a range of JET discharge scenarios. To obtain adequate statistical accuracy, it was often necessary to aggregate the spectra over numbers of similar discharges. The groups of discharges include the following scenarios:-

- (i) the three highest fusion power (42676, 42974 and 42976) hot ion H-mode discharges with about 20 MW NBI and up to 4 MW ICRH heating power. During the high performance phase, we find $T_{\perp} \approx 1.5 \times T_{\parallel}$, and $T_{\parallel} \approx T_i$ (CXRS).
- (ii) optimized shear discharges (numbers 42741, 42743, 42746, 42750, 42751, 42915, 42938, and 42939), with central ion temperatures above 20 keV, using 20 MW of NBI and 6 to 7 MW of ICRH power. Unusually, at peak performance we find $T_{\perp} \approx T_{\parallel} \approx T_i$ (CXRS), indicating very strong thermal neutron emission.
- (iii) ICRF heated discharges [16] with ^3He minority and tritium second harmonic ICRH ($\omega = 37$ MHz, toroidal field equal to 3.7 T) for which the d-t neutron production rate was higher than 10^{17} n/s. This permitted the accumulation of ~ 250 counts in $^{12}\text{C}(n,\alpha_0)^9\text{Be}$ line of the NDD4 and NDD5 pulse height spectra from two discharges of 10 seconds duration with ^3He minority heating and ~ 150 counts with tritium second harmonic heating. The neutron temperatures were ~ 12 keV and ~ 6 keV, respectively. For these cases $T_{\perp} \approx T_{\parallel} \approx T_i$ (CXRS), as expected in the absence of strong populations of accelerated particles.
- (iv) ρ^* scaling experiments (42993, 43002, 43003, 43004, and 43005) with about 12 MW of pure tritium NBI, for which $T_{\perp} \approx 1.5 \times T_{\parallel} \approx 32$ keV, whereas the measured temperature of the thermal ions was just 4 keV.

(v) the α -particle heating experiment [17], using 3.8 MA/3.4T hot ion H-mode discharges with 11 MW NBI and edge localized mode (ELM)-free periods of about 2.5 s and sawtooth periods of more than 1 s. A 5-point tritium to deuterium density ratio scan was performed from pure deuterium, through the optimum \sim 50-50 mixture with fusion power of about 6.7 MW, to nearly pure tritium. Once more, we find $T_{\perp} \approx 1.5 \times T_{\parallel}$, and $T_{\parallel} \approx T_i$ (CXRS). No significant differences in neutron temperature were apparent from the diamond spectrometers for these five discharges.

In figs. 6-10 we compare the neutron temperatures for the above discharges as determined by neutron spectrometers using the various lines-of-sight. Fig. 6 compares PRTel neutron temperatures with those determined the MPR, for comparable lines-of-sight. The agreement is excellent, apart from in the range 10 to 15 keV; these discrepancies are almost certainly due to the PRTel line-of-sight passing 15 cm below the plasma core. (Temperatures below 20 keV were measured either for plasmas heated with ICRF or were obtained after neutral beam-heating had been discontinued. In both instances, the plasma temperature profiles become very sharply peaked and PRTel would be expected to give temperatures 10 to 20% lower than the MPR).

In fig. 7 the neutron temperatures derived from the two diamonds NDD1 and NDD4 are compared with those derived from PRTel. All three spectrometers share the same tangential-viewing line-of-sight and should return identical results. The main observation is that the error bars associated with the diamond detectors increase with neutron temperature so that it becomes impractical to use them for neutron spectrometry for plasmas with very high neutron temperatures.

In fig.8 the neutron temperatures obtained from the diamond detector NDD5 and TANSY are compared; these spectrometers both have vertical lines-of-sight. Both spectrometers return rather large uncertainties, with those from TANSY being marginally smaller. The results are broadly similar.

Figs. 9 and 10 contrast the neutron temperatures measured with vertical and tangential lines-of-sight. The most accurate comparison is obtained from TANSY and the MPR, although diamond NDD5 could be substituted for TANSY with little loss of accuracy. The comparison of vertical-viewing diamond with the tangential-viewing diamond is spoiled by the large uncertainties

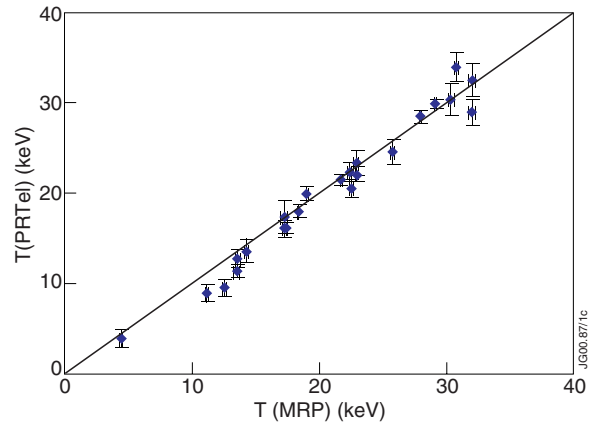


Fig.6: Neutron temperatures determined from neutron spectra obtained with the annular-radiator proton recoil spectrometer (PRTel) compared with the results obtained with the magnetic analysis proton recoil spectrometer (MPR). These two spectrometers have similar, but not identical, tangential lines-of-sight. Good agreement between the two types of spectrometer is evident. In this and later figures, the neutron spectra are assumed to be Gaussian and the results are “neutron temperatures” deduced directly from the fwhm values, without regard to the need to distinguish beam-plasma from thermal reactions

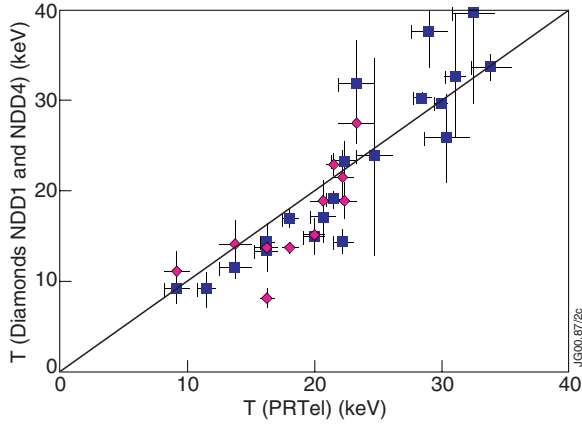


Fig.7: Neutron temperatures determined from neutron spectra obtained with diamond detectors NDD1 And NDD4 compared with results obtained with the annular-radiator proton recoil spectrometer (PRTel). These spectrometers all share the same tangential line-of-sight. The temperatures from the two diamonds show a tendency to be lower than the PRTel values and the accuracy degrades with increasing temperature; both effects are attributable to inadequate knowledge of the diamond detector response functions.

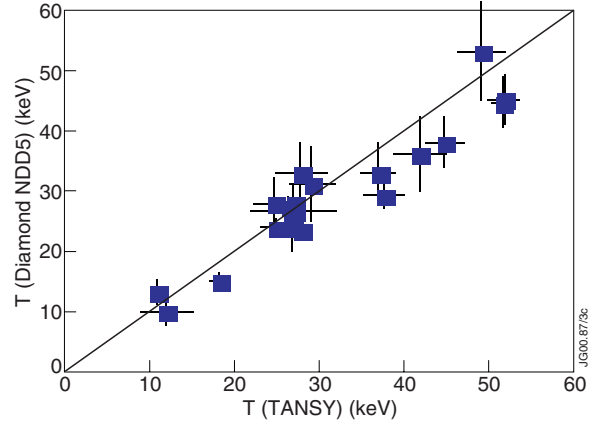


Fig.8: Neutron temperatures determined from neutron spectra obtained with diamond detector NDD5 compared with results obtained with the associated-particle time-of-flight spectrometer ((TANSY). These spectrometers utilize similar vertical lines-of-sight. The temperatures from the diamond do show a tendency to be about 10% lower than the TANSY values, although the statistical errors are quite high.

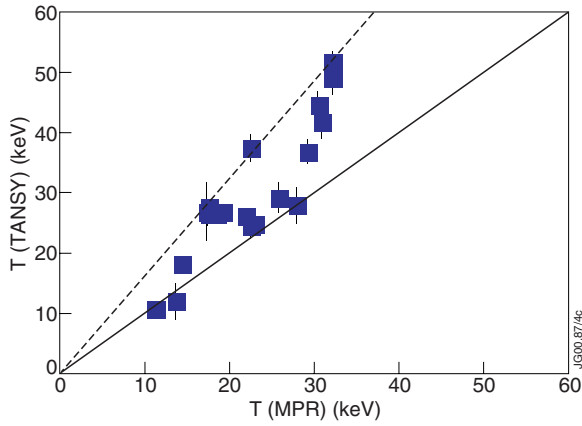


Fig.9: Neutron temperatures determined from neutron spectra obtained with the associated-particle time-of-flight spectrometer (TANSY), utilizing a vertical line-of-sight, compared with the results obtained with the magnetic analysis proton recoil spectrometer (MPR), utilizing a tangential line-of-sight. As expected, the data points fall between lines representing a fast-ion velocity distribution that is perpendicular to the magnetic field lines (dotted) and one that is isotropic (solid).

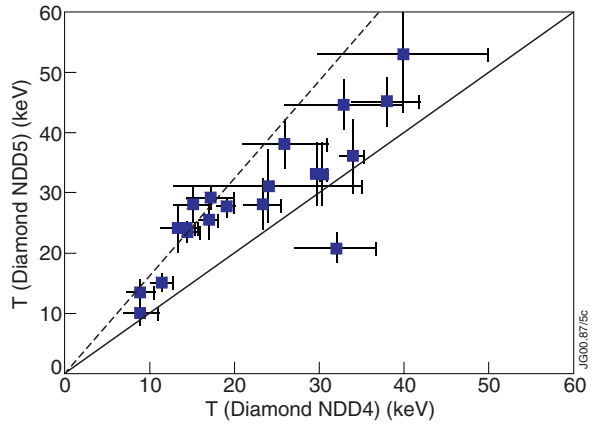


Fig.10: Neutron temperatures determined from neutron spectra obtained with diamond NDD5, utilizing a vertical line-of-sight, compared with the results obtained with diamond NDD4, utilizing a horizontal line-of-sight. As in fig. 9, the data points fall between lines representing a fast-ion velocity distribution that is perpendicular to the magnetic field lines (dotted) and one that is isotropic (solid). However, the error bars are quite large, especially for the tangential line-of-sight.

associated with the latter, NDD4. The data-points should all fall between the two lines, provided $T_{//} < T_{\perp}$. The slope of the upper line is $(\sin^2 52)^{-1}$.

With ICRF heating, we naturally expect $T_{//} \sim T_i(\text{CXRS})$. Because of the oblique beam injection angle, we also expect this relation to apply approximately to the beam-heating case.

6. CONCLUSIONS

High energy resolution natural diamond detectors were successfully used for monitoring the d-t neutron emission rate during the 1997 JET tritium experiments and for measurements of the perpendicular and tangential d-t neutron spectra.

The spectrometers permitted neutron temperatures to be derived from the d-t neutron energy distributions for plasma regimes associated with strong neutron emission; when the thermal neutron emission is dominant, e.g. during optimized shear experiments, the neutron temperatures and the thermal ion temperatures coincide.

The potential of diamond detectors for neutron spectrometry in future fusion devices has been studied by comparison with the performance of the major neutron spectrometers installed at JET. In general, their performance at JET cannot be considered competitive with that of the major spectrometers. Due to the existence of nuclear reaction channels other than the desired $C(n,\alpha_0)^9\text{Be}$ channel and to incomplete charge collection, the response function for NDD (and the procedure of neutron spectrum unfolding) is more complicated than it is for the major spectrometers. However, their high energy resolution, high radiation resistance and small size, together with their ability to operate at high count rates, indicates their suitability for d-t neutron measurements in future fusion reactors, with particular relevance for multichannel d-t neutron spectrometry.

REFERENCES

- [1] M.Keilhacker, A.Gibson, et al., and the JET Team, Nuclear Fusion **39** (1999) 209.
- [2] Konorova,E.A., Kozlov,S.F., Sov. Phys. Semiconductors **4**, (1971) 1600.
- [3] Lchanskii,A.E., Martynov,S.S., Khrunov,V.S., Cheklaev,V.A. Sov. Atomic Energy **63**, (1987) 639.
- [4] Krasilnikov,A.V., Amosov,V.N. and Kaschuck,Yu.A., Trans.Nucl.Sci., **45** (1998) 385.
- [5] Krasilnikov,A.V., Roquemore,A.L., Gorelenkov,N.N., Budny, R.V., Fusion Energy 1996. Proceedings of 16th International conference on Fusion Energy organized by the IAEA Montreal 7-11 October 1996, v.1, (1997) p.293-301.
- [6] Krasilnikov A.V., in "Diagnostic for ITER" P.E.Stott, et.al. editors, p.435, Plenum Press, New York and London, (1995).
- [7] Kaschuck Yu.A., Portnov D.V., Amosov V.N.,Krasilnikov A.V. and Siromukov S.V., Rev. Sci. Instrum., **70**, 1104, 1999.
- [8] N.P.Hawkes, P. van Belle, D.S.Bond, S.Croft and O.N.Jarvis, Rev.Sci.Instrum. **70** (1999) 1134.
- [9] Swinhoe, M.T and Jarvis, O.N, Rev Sci Instr **56** (1985) 1093.
- [10] Brysk,H., Plasma Physics **15** (1973) 611.
- [11] Cordey J.G., Balet B., Bartlett D.B., et.al., Nuclear Fusion, **39** (1999) 301.
- [12] Van Belle P. and Sadler G. "The computation of fusion product spectra from high

temperature plasmas” in Basic and advanced fusion plasma diagnostic techniques, Varenna 1986, v. III, EUR 10797 EN (1986) 764-774.

- [13] Grosshög G., et.al., Nucl. Instrum. & Methods, **A249**, (1986) 468.
- [14] S.Conroy, G.Ericsson et al., “Neutron emission reference characterization of selected JET DT discharges, based on MPR spectrometer measurements”, Uppsala University Report UU-NF99#9 (Dec.1999).
- [15] J.Kallne et al, Rev. Sci. Instrum. **70** (1999)1181.
- [16] Start D.F.H., et.al., Nucl.Fusion, **39** (1999) 321.
- [17] Thomas P.R. et.al., Phys.Rev.Lett. **80** (1998) 5548.